

The Thermodynamics of Endosomal Escape and DNA Release from Lipoplexes

Yotam Y. Avital,^{1,2} Niels Grønbech-Jensen,^{3,4} and Oded Farago^{1,2}

¹*Department of Biomedical Engineering, Ben-Gurion University of the Negev, Be'er Sheva 85105, Israel*

²*Ilse Katz Institute for Nanoscale Science and Technology,
Ben-Gurion University of the Negev, Be'er Sheva 85105, Israel*

³*Department of Mechanical and Aerospace Engineering,
University of California, Davis, California 95616, USA*

⁴*Department Mathematics, University of California, Davis, California 95616, USA*

Complexes of cationic and neutral lipids and DNA (lipoplexes) are emerging as promising vectors for gene therapy applications. Their appeal stems from their non pathogenic nature and the fact that they self-assemble under conditions of thermal equilibrium. Lipoplex adhesion to the cell plasma membrane initiates a three-stage process termed transfection, consisting of (i) endocytosis, (ii) lipoplex breakdown, and (iii) DNA release followed by gene expression. As successful transfection requires lipoplex degradation, it tends to be hindered by the lipoplex thermodynamic stability; nevertheless, it is known that the transfection process may proceed spontaneously. Here, we use a simple model to study the thermodynamic driving forces governing transfection. We demonstrate that after endocytosis [stage (i)], the lipoplex becomes inherently unstable. This instability, which is triggered by interactions between the cationic lipids of the lipoplex and the anionic lipids of the enveloping plasma membrane, is entropically controlled involving both remixing of the lipids and counterions release. Our detailed calculation shows that the free energy gain during stage (ii) is approximately linear in Φ_+ , the mole fraction of cationic lipids in the lipoplex. This free energy gain, ΔF , reduces the barrier for fusion between the enveloping and the lipoplex bilayers, which produces a hole allowing for DNA release [stage (iii)]. The linear relationship between ΔF and the fraction of cationic lipids explains the experimentally observed exponential increase of transfection efficiency with Φ_+ in lamellar lipoplexes.

Somatic gene therapy holds great promise for future medical applications including, for example, new treatments for various inherited diseases and cancers [1]. Within this approach, an attempt is made to replace damaged genes with properly functioning ones. The core of the process, called transfection, includes the key steps of transferring foreign DNA into a target cell, followed by expression of the genetic information. Complexes composed of cationic lipids (CLs) and DNA, designated lipoplexes, constitute one of the most promising non-viral gene delivery systems [2–4]. Though their transfection efficiency (TE) is, in general, inferior to that of viral vectors, lipoplexes have the advantage of triggering low immune response, and being non-pathogenic [4–7]. Furthermore, lipoplexes allow transfer of larger DNA segments. Their production does not require sophisticated engineering, since they form spontaneously in aqueous solutions when DNA molecules are mixed with CLs and neutral lipids (NLs) [8–11]. The main thermodynamic driving force for lipoplex formation is the entropic gain stemming from the release of the tightly bound counterions from the DNA and the lipid bilayers. X-ray diffraction experiments have revealed several liquid crystalline phases of CL-DNA complexes. The two most prominent structures are: (i) a lamellar phase (L_α^C), with 2D smectic array of DNA within lipid bilayers [8], and (ii) an inverted hexagonal phase (H_{II}^C), where the DNA rods are packed in hexagonal lattice and the lipids form monolayers around them [9].

Isoelectric complexes, where the total charge on the DNA molecules exactly matches the total charge of the

CLs, are the most stable ones because they enable nearly complete counterion release [12]. The thermodynamic stability of a lipoplex, however, is only one of several biophysical parameters affecting the TEs of lipoplexes. Another parameter is the liquid crystalline structure of the complex [13], which is largely determined by the bending rigidity and spontaneous curvature of the lipids [14]. Generally speaking, H_{II}^C complexes exhibit higher TEs than L_α^C complexes. A third parameter is the charge density (per unit area) of the lipoplex membranes, which can be varied by mixing different ratios of CLs and NLs, and by using multivalent CLs [15].

Further improvement of the therapeutic efficacy of lipid vectors requires better understanding of their mechanism of transfection, and the biophysical parameters of the CL-DNA complexes that influence it. Transfection is viewed as a three-stage process starting with adsorption and entry (via endocytosis) of the CL-DNA complex into the cell, followed by lipoplex degradation, and finally ending with the release of the DNA, making the latter available for expression [13, 16, 17]. The first stage is driven by electrostatic attraction between the lipoplex CLs and the negatively charged lipids of the cell plasma membrane, which enables further release of counterions (see discussion below). After endocytosis the complex is within the cell, trapped inside an endosome. The second stage of the transfection process, which often emerges as the rate-limiting one, involves breakdown of CL-DNA complex. During this stage, the endosomal and the lipoplex external membranes fuse [13]. It has been speculated that the improved TE of hexagonal complexes

over lamellar ones stems from its lower energy barrier of fusion [13]. In the case of lamellar complexes, the fusion energy barrier decreases (and TE increases) when the mole fraction of CLs increases. These observations suggest that the electrostatic attraction between the lipoplex and the endosomal membrane triggers a thermodynamic instability leading to morphologic changes. In this work we explore the thermodynamic driving forces governing the transfection process from the stage of adhesion and endocytosis, up to the stage of DNA release.

CL-DNA complexes adhere to cell membranes due to considerations similar to those triggering their formation, namely counterion release. Both the plasma membrane and the external bilayer of the lipoplex are covered with layers of tightly bound counterions [fig. 1(A)]. These counterions neutralize the lipid charges, and exclude the electric field from the oily parts of the membranes. The loss of positional entropy of the bound counterions is significantly lower than the energetic cost of allowing an electric field to penetrate the bilayers low dielectric hydrophobic core. When the oppositely charged surfaces are in close proximity, the anionic and cationic lipids can neutralize each other, which enables the release of counterion pairs. The positional entropy gained by the released counterions is the main driving force for cell-lipoplex adhesion which initiates cellular entry via endocytosis.

Figure 1(B) shows, schematically, a small segment of a lipoplex trapped within an endosome. The entrapped lipoplex represents a thermodynamic system that is substantially different from the lipoplex originally residing outside the cell. The difference stems from the presence of anionic lipids (ALs) in the plasma membrane which can now mix with the CLs and NLs of the lipoplex [13]. The process of lipid mixing is slow since it requires the lipids to “flip-flop” between monolayers; nevertheless, it encompasses a large entropic reward. Moreover, redistribution of the lipids, while protecting the hydrophobic cores of the bilayers from electric fields, dictates that the counterions “escort” the flip-flopping charged lipids. When ions move between the different aqueous layers of the system they meet oppositely charged ions which allows them to mutually leave the system without affecting its charge neutrality.

The considerations presented in the previous paragraph suggest that the entrapment of a lipoplex by the endosome may be sufficient to render it thermodynamically unstable. This is obviously a desirable feature since the ultimate goal of the transfection process is lipoplex disassembly and DNA release. To better understand the thermodynamics of transfection, we will present a simplified model where electrostatic interactions are considered within the framework of a mean field approximation. The model treats the membranes, as well as the DNA array, as uniformly charged planar sheets [fig. 1(C)].

Before describing the model, let us return to figure 1(B) illustrating the entrapped lipoplex immediately after endocytosis. The system constitutes six charged layers. In reverse order [from number 6 to 1, see fig. 1(B)],

these charged layers correspond to: 6 - the lipid monolayer “below” the DNA array, 5 (also denoted by D) - the DNA array, 4 - the lipid monolayer “above” the DNA array, 3 and 2 - the “intermediate” lipid monolayers, and 1 - the lipid monolayer facing the cytoplasm. The three aqueous environments in the system will be denoted by: 1 - the cytoplasm, 2 - the intermediate thin water layer between the endosomal membrane and the lipoplex, and 3 - the internal water region surrounding the first DNA layer. At the initial state, the lipid composition in monolayers 1 and 2 is that of the cell plasma membrane. It consists of ALs and NLs only and, for simplicity, will be assumed to be symmetric. Similarly, surfaces 3-6 are in the equilibrium state of the self-assembled lipoplex, and have the same CL to NL ratio. We will also assume that the NLs of the plasma and lipoplex membranes are of the same type.

The three major contributions to the free energy of the system arise from electrostatic interactions, lipid mixing entropy, and the entropy loss of bound counterions. In our model system, fig. 1(C), the lipid monolayers are replaced with uniformly charged flat surfaces of charge density σ_i ($i=1,2,3,4,6$). The aqueous solutions have a dielectric constant $\epsilon_w \simeq 80$, while that of the hydrophobic regions, ϵ_o is assumed to be vanishingly small. This precludes the penetration of electric fields into the hydrophobic regions due to the associated very large electrostatic energy [20, 21]. (We note that the cytoplasm is occupied with concentrated macromolecules. Their presence changes the inside relative permittivity to values ranging from about 50 to over 200 [18, 19], for which the assumption concerning the exclusion of the electric field is from the hydrophobic regions still holds.) A somewhat greater approximation that we make is replacing the electric field of the DNA array with the electric field of a flat surface of charge density per unit area $\sigma_5 = \lambda/d_{\text{DNA}}$ where $\lambda \simeq 1.7e/\text{\AA}$ is the linear (per unit length) charge density of the DNA rod, and d_{DNA} is the inter-DNA spacing. A more detailed mean field calculation, taking into account the geometry of the DNA rods, can be performed computationally [12]. Such a calculation, however, is not necessary here. In order to understand the “big picture”, one only needs to recognize that the counterions must arrange themselves to minimize the electrostatic energy. Any appreciable deviation in the ions distribution will involve an energy cost much larger than the entropic components of the free energy. Specifically for the model system in fig. 1(C), the number of ions per unit area present in each aqueous environment will have to match the area charge densities of the surfaces in a manner that eliminates the electric field from the low dielectric regions [22]. Electric field can be present in the aqueous regions, and the associated energy can be derived by integrating over the electrostatic energy density. Under no-salt conditions, this precisely gives the free energy cost attributed to the bound counterions. We will not perform the exact calculation (which requires the solution of a corresponding Poisson-Boltzmann equation), but instead employ a

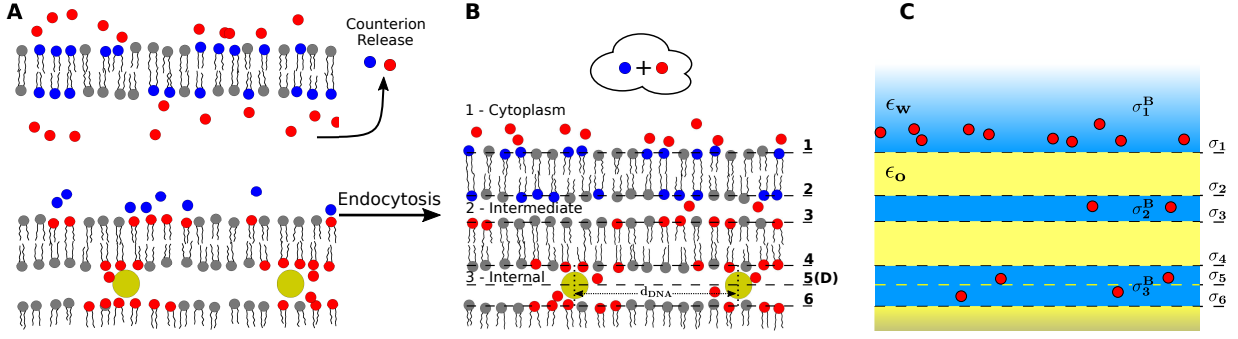


FIG. 1: **(A)** Schematics of a complex of CLs (head groups depicted as red circles), NLs (head groups - grey circles), and DNA rods (larger yellow circles), separated from the plasma membrane which is composed of ALs (head groups - blue circles) and NLs. The lipoplex attracts a layer of bound anions (shown as blue circles), while the plasma membrane is surrounded by bound cations (red circles). **(B)** The state of the system after adhesion and endocytosis, the formation of which is driven by cation-anion pairs release. **(C)** A simplified model of the system depicted in **B** (see detailed explanation in text). The model system consists of 6 uniformly charged plates with charge density σ_i and three water layers (shown in blue) where the ions reside. The yellow stripes represent hydrophobic regions that do not include ions, and at which the electric field must vanish. Notice that the 5th charged plate, which represents the DNA array, allows crossover of ions.

simple approximation and assign each bound counterion with a free energy of $1k_B T$ [12, 23].

Let us denote by ϕ_i^+ , and ϕ_i^- the mole fractions of the cationic and anionic lipids in monolayer i , respectively, where the monolayers are located at z_i . The area per lipid, a , is taken as identical for all three lipid species (CLs, ALs, and NLs). We denote by n^+ and n^- the number densities, per unit volume, of the cations and anions, respectively. To make the mean field approximation applicable, we consider the case where all the charged lipids, as well as the counterions, are monovalent. Assuming ideal lipid mixing in the monolayers, the uniform charge density of each surface is $\sigma_i = e(\phi_i^+ - \phi_i^-)/a$ where e is the electron charge. Since the system has a planar symmetry in the $x-y$ plane, the electric field at any point must be orthogonal to the plane, i.e., along the z axis. Moreover, $n^+ = n^+(z)$, $n^- = n^-(z)$, and both vanish inside the hydrophobic parts of the membranes [colored in yellow in fig. 1(C)] where $\epsilon_o \ll \epsilon_w$. The electric field at a given coordinate z is given by $E_z = \tilde{\sigma}/2\epsilon_z$ where

$$\begin{aligned} \tilde{\sigma} &= \\ &= e \int_{-\infty}^z \left[n^+(z') - n^-(z') + \sum_{i=1}^6 \sigma_i \delta(z' - z_i) \right] dz' \\ &- e \int_z^{\infty} \left[n^+(z') - n^-(z') + \sum_{i=1}^6 \sigma_i \delta(z' - z_i) \right] dz' = \\ &= 2e \int_{-\infty}^z \left[n^+(z') - n^-(z') + \sum_{i=1}^6 \sigma_i \delta(z' - z_i) \right] dz', \end{aligned} \quad (1)$$

and ϵ_z is the dielectric constant at z . The second equality in eq. (1) is due to the overall charge neutrality of the system.

The requirement that the electric field vanishes inside the low dielectric regions of the bilayers can be used to

determine, via eq. (1), the number of bound counterions, N_j^B , in the three aqueous solutions of the system ($j = 1, 2, 3$). In each such region we expect to find only one type of counterions since pairs of oppositely charged counterions can be released without affecting the charge balance. Defining $\sigma_j^B = s_j e (N_j^B/a)$, where $s_j = +1$ ($s_j = -1$) for cations (anions), the number of counterions bound to the endosome on its cytoplasmic side is calculated through

$$\sigma_1^B = -\sigma_1. \quad (2)$$

This relation ensures that the electric field between layers $i = 1$ and $i = 2$ vanishes. By the same logic, in the intermediate water layer

$$\sigma_2^B = -(\sigma_1 + \sigma_2 + \sigma_3 + \sigma_1^B) = -(\sigma_2 + \sigma_3), \quad (3)$$

and in the internal water layer

$$\sigma_3^B = -(\sigma_4 + \sigma_5 + \sigma_6). \quad (4)$$

At short times after cellular intake, the surface charge densities of the endosome layers, σ_i , match those of the cell plasma membrane ($i = 1, 2$), and the lipoplex ($i = 3 - 6$). This initial state is, however, no longer the equilibrium state, since the anionic and cationic lipids can now mix with each other. This occurs via slow, but steady, “flip-flopping” events switching lipids between monolayers $i = 1 - 4$ [24]. The redistribution of lipids between these monolayers not only increases the mixing entropy of the lipids within the layers, but may also allow further release of counterions whose densities within the aqueous solutions are simultaneously updated in order to satisfy the conditions of eqs. (2)-(4). Taking these considerations into account, we write the total free energy of the system, per unit area of the lipids a , as

$$\frac{F}{ak_BT} = \sum_{i=1}^4 [\phi_i^+ \log(\phi_i^+) + \phi_i^- \log(\phi_i^-) + (1 - \phi_i^+ - \phi_i^-) \log(1 - \phi_i^+ - \phi_i^-)] + \sum_{j=1}^3 N_j^B, \quad (5)$$

where ϕ_i^\pm are the mole fractions of cationic (+) and anionic (−) lipids at the i -th layer, and N_j^B is the number of bound counterions per unit area a at the j -th water layer (see definitions also above). The first term in eq. (5) accounts for the mixing entropy of the lipids in each monolayer, while the second term represents the entropy cost of bound counterions. The former is based on the mean field assumption of ideal mixing. The latter employs the commonly used assumption of $1k_BT$ per bound counterion.

Let $\{\phi_{i,0}^\pm\}$ denote the initial mole fractions of the CLs and ALs. To find the equilibrium state, we need to minimize the free energy in eq. (5) with respect to the variables $\{\phi_i^\pm\}$, under the constraints that $\sum_{i=1}^4 \phi_i^+ = \sum_{i=1}^4 \phi_{i,0}^+$, and $\sum_{i=1}^4 \phi_i^- = \sum_{i=1}^4 \phi_{i,0}^-$ representing the preservation of the total number of lipids of each type. The dependence of $\{N_j^B\}$ on the variables $\{\phi_i^\pm\}$, is given by eqs. (2)-(4), where $N_j^B = (a/e)|\sigma_j^B|$, and $\sigma_i = e(\phi_i^+ - \phi_i^-)/a$. Notice that in contrast to the lipids, the total number of bound counterions is not fixed but may vary by intake or release of ions from the cytoplasm.

The free energy ΔF , per unit area a , that the system may gain during stage (ii) of the transfection process is given by the difference in F [eq. (5)] between the equilibrium and initial states. In the initial state, the distribution of lipids in the plasma membrane is given by $\phi_{i,0}^- = \Phi_-$ and $\phi_{i,0}^+ = 0$, for $i = 1, 2$. In the lipoplex membranes ($i = 3, 4, 6$), $\phi_{i,0}^- = 0$ and $\phi_{i,0}^+ = \Phi_+$. For convenience, we define the “mole fraction”, $\Phi_D = -(a/e)\sigma_5$, associated with the DNA array. Figure 2(A) plots our results for ΔF as a function of $q = 2\Phi_+/\Phi_D$, which is the lipoplex charge ratio. The ratio q is varied by changing Φ_+ , while keeping $\Phi_D = 1$ fixed. We also fix Φ_- , the initial anionic lipid mole fraction in the plasma membrane, to 0.5. The data for ΔF is plotted in solid line, while the dotted and dashed curves show, respectively, the partial contributions due to lipid mixing [first term in eq. (5)] and the bound counterions (second term). The results reveal the existence of three different regimes. In regime (i), corresponding to $q < 1$, the decrease in ΔF with q is very slow, and arises exclusively from the lipid mixing term. In regime (ii) where $1 < q < 4/3$, the decrease in ΔF is faster due to the additional contribution of counterion release. Finally, in regime (iii) where $q > 4/3$, lipid mixing becomes again a dominant factor, though there is a fixed gain of entropy due to counterion release.

The key to understand the trends in fig. 2(A) is to correctly identify the transition points between the three different regimes. The transition from (i) to (ii) occurs at $q = 1$, which is the isoelectric point of the lipoplex,

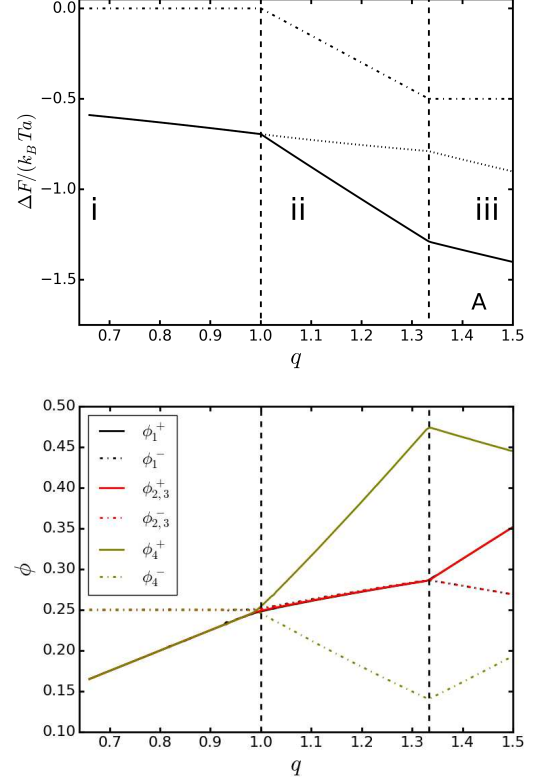


FIG. 2: (A). Solid line - the free energy ΔF (see text for definition), as a function of $q = 2\Phi_+/\Phi_D$ with $\Phi_D = 1$ and $\Phi_- = 0.5$. Dot-dashed and dotted lines show the partial contributions to ΔF originating, respectively, from counterion release and lipid mixing. (B). The equilibrium distribution of CLs (solid lines) and ALs (dot-dashed lines) in monolayers $i = 1$ (black), $i = 2, 3$ (red) and $i = 4$ (yellow). The vertical dashed lines mark the transition points between the different regimes discussed in the text.

namely the point where the total cationic charge of the lipids *exactly* matches the negative one of the DNA array: $2\Phi_+ = \phi_D$. Therefore, in regime (i) ($q < 1$), the internal solution surrounding the DNA array includes cations [see eq. (4)]. Similarly, the external solution facing the cytoplasm, and the intermediate solutions between the plasma membrane and the lipoplex, also include cations only [eqs. (2) and (3)]. Since the system contains no anions, it is impossible to release cation-anion pairs, which explains why, in this regime, the only contribution to the free energy comes from mixing of the lipids. Equilibrium is achieved when the lipids are evenly distributed between the four monolayers. In contrast to regime (i), in

regime (ii) ($1 < q < 4/3$) both the intermediate and the internal solutions include anions at the initial conditions, while the external solutions contains cations. Therefore, the decrease in free energy now involves contributions of both lipid mixing and counterion release. Detailed calculation shows that in regime (ii), equilibrium is reached when all the anions are released, while the excess cations accumulate at the internal water layer around the DNA molecules. Moreover, to satisfy the conditions of eqs. (2) and (3), the net charge density σ_i in monolayers $i = 1, 2, 3$ must vanish, which means that the mole fractions of CLs and ALs in each of these layers are the same. The composition of layer $i = 4$ is different, which implies that lipid mixing is not optimized in regime (ii). Regime (ii) ends at $q = 4/3$, which is the point where the total charge of the system (including the ALs of the plasma membrane, the CLs of the lipoplex, and the DNA array) vanishes; i.e., when

$$3\Phi_+ = \Phi_D + 2\Phi_- \quad (6)$$

Therefore, at this point, the total numbers of bound cations and anions is also the same. Further increasing q , by increasing the fraction of the CLs and the number of associated bound anions, we enter into regime (iii). In this regime, the total gain of free energy due to counterion release saturates, since it is capped by the number of cations originally bound to the plasma membrane. The free energy ΔF continues to decrease with q since the lipids can now better mix and attain a more even distribution between monolayers $i = 1 - 4$. The equilibrium distribution of lipids between the four monolayers are depicted in fig. 2(B). Notice that the composition of lipids in monolayers $i = 2, 3$ is always the same, which is anticipated since any exchange of lipids between these two monolayers will not influence the charge balance condition of eq. (3).

Figure 3(A) depicts our results for ΔF for a lipoplex with more densely packed DNA rods ($\Phi_D = 1.4$). The charge density of the plasma membrane is the same as in fig. 2(A), $\Phi_- = 0.5$. The characteristics of fig. 3(A) are very similar to the those observed in fig. 2(A). One noticeable difference is that regime (ii) starts below the isoelectric point $q < 1$, at $q = \Phi_D^{-1} \simeq 0.71$. As in the previously discussed case, in regime (i) the initial state of the system includes only cations. In regime (ii) the intermediate water layer contains anions, which are released upon reaching equilibrium. The kink at the isoelectric point is due to the fact that for $q > 1$, the internal solution also contains anions. The transition between regions (ii) and (iii) is at $q \simeq 1.14$, as dictated by eq. (6). In regime (iii), the contribution of counterions release to ΔF is fixed by the amount of cations present in the system.

Figure 3(B) depicts our results for ΔF for a lipoplex with more loosely packed DNA rods ($\Phi_D = 0.6$), with a plasma membrane of charge density $\Phi_- = 0.5$. Here, the transition from (i) to (ii) is at the isoelectric point $q = 1$ which, as noted above, is where anions first appear at the

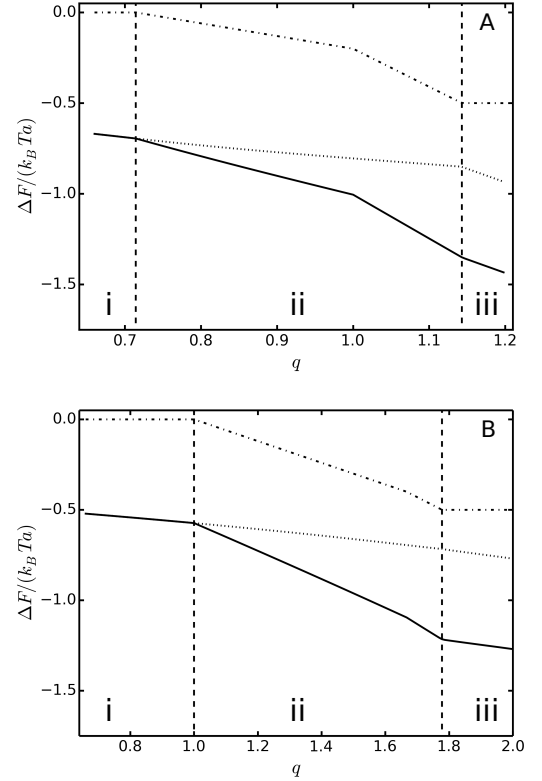


FIG. 3: (A) The free energy ΔF (solid line) and the partial contributions to ΔF originating from counterions release (dot dashed line) and lipid mixing (dotted line). Results are for a lipoplex with densely packed DNA molecules ($\Phi_D = 1.4$). The vertical dashed lines marks the transition points between the regimes discussed in the text. (B) Same as in (A) for a lipoplex with loosely packed DNA molecules ($\Phi_D = 0.6$).

internal layer next to the DNA. The kink happens at $q = \Phi_D^{-1} \simeq 1.67$ above which, the intermediate water layer contains anions at the initial state. The transition from (ii) to (iii) occurs at $q \simeq 1.78$, as predicted by eq. (6).

The free energy calculations reported in figs. 2 and 3 demonstrate the inherent instability of the entrapped lipoplex, triggered by its interactions with the enveloping plasma membrane. The latter constitutes a reservoir of ALs that can mix with the CLs of the lipoplex. Lipid mixing occurs through “flip-flop” events which, in general, are slow especially when lipids transfer between distinct bilayers (as opposed to lipids moving between monolayers of the same membrane, which is probably somewhat faster). The exchange of lipids between the plasma and lipoplex membranes may cause these two membranes to fuse [13] - a scenario that we have thus far not taken into account. Fusion is thermodynamically favorable since it reduces the number of participating monolayers from $i = 4$ to $i = 2$ and, thus, it further increases the lipid mixing entropy. However, it comes with the cost of bending energy. Crossing the associated energy barrier is what primarily determines the rate of

successful endosomal escape and sets the TE (transfection efficiency). Experimentally, it is known that the TE of lamellar complexes grows exponentially with the cationic charge density of the complex, $\Phi_+ = (q\Phi_D)/2$. This observation supports the picture of activated fusion where $TE \sim \exp(-\Delta F/k_B T)$, and

$$\Delta F = a\kappa - b\Phi_+ + c, \quad (7)$$

where κ is the bending rigidity of the bilayers, while a , b , and c are parameters, the value of which may depend on the molecular conditions inside the endosome (see eq. (2) in [13]). The first term in eq. (7) represents the curvature energy cost of the fusion which, to a good approximation, is independent of the charge densities. The second term has been previously attributed to the electrostatic attraction between the plasma membrane and the complex. The last term accounts for other effects, e.g., the capacity of the low-pH environment of the endosome to disrupt the lipid bilayer. Our study reveals that the origin of second term is actually *not* energetic but entropic. The free energy gain ΔF due to lipid mixing and the associated counterion release at the second stage of the transfection process (see solid curves in fig. 2 and 3) grows piecewise linearly with Φ_+ . This linear dependence is simply a reflection of the fact that when the lipoplex contains a higher fraction of CLs, the potential entropic gain involved in ideal mixing of lipids and counterions release is larger.

Once fusion occurs, a hole opens that connects the cytoplasm and the internal water layer containing the first DNA array of the lipoplex. This allows for influx of positively charged (macro)molecules, e.g., unstructured peptides, that are able to condense the DNA molecules and release them to the cytoplasm [25]. Removing the first DNA layer leaves us with a smaller lipoplex whose composition is similar to the original one. Interactions of this positively charged complex with negatively charged components of the cell may cause renewed thermodynamic instability and lead to further degradation of the CL-DNA complex.

To conclude, we use a simplified model to study the thermodynamics of transfection by CL-DNA complexes (lipoplexes). The formation of these complexes is known to be driven by the increase in the translational entropy of the counterions that are released to the bulk solution when the oppositely charged membranes and DNA molecules associate together. The same counterion release mechanism mediates (at least partially) the adhesion of the lipoplex to the cell plasma membrane, which initiates the transfection process. In this work, we argue that the contact between the lipoplex external bi-

layer and the plasma membrane triggers thermodynamic instability that leads to lipoplex degradation, which is essential for the transfection process to proceed. The thermodynamic instability of the entrapped lipoplex is of entropic origin: It stems from the fact that the lipid composition of the lipoplex and the plasma membrane is different and, therefore, mixing of these lipids increases the configurational entropy of the system. Since the two membranes are oppositely charged, the mixing of lipids has another effect - it reduces the charge density of the membranes. This enables further counterion release and a further decrease in the free energy. Thus, the counterion release mechanism which has been identified as the thermodynamic driving force for formation of various supramolecular structures [26], is here used to explain the disassembly of such structures.

Despite the gross simplicity of our model and the fact that it ignores specific molecular details, it successfully predicts a roughly *linear* increase in the free energy gain with the mole fraction of CLs in the complex, which explains the observed *exponential* increase in transfection efficiency of lamellar complexes with the charge density. The model is based on a mean-field picture and replaces the lipid monolayers with uniformly charged flat surfaces. This modeling approach is routinely used in theoretical studies of electrostatic effects in soft matter systems. We avoid solving the Poisson-Boltzmann (PB) equation explicitly, and instead associate each released counterion with a free energy gain of $1k_B T$. By solving the PB equation, a more accurate value may be obtained (which may depend on the water layer from where the counterion is released), but the result is only expected to be different by a factor of order unity. What might be the boldest approximation in our model is the replacement of the DNA array with a uniformly charged surface as well. By employing this picture, we essentially ignore two entropic contributions of opposite sign: (i) The CLs in the monolayers facing the DNA arrays are expected to accumulate near the DNA rods, which lowers their mixing entropy. (ii) The space available to the ions surrounding the DNA molecules is quite small, which implies that the entropic gain involving in their release may be higher than assumed by the model. The order of magnitude of these effects is comparable to the other contributions discussed here. Therefore, although we do not expect these two entropic contributions to cancel each other, we also do not expect them to dominate and modify the picture presented here.

This work was supported by the Israel Science Foundation (ISF) through grant no. 1087/13.

[1] N. Smyth-Templeton and D. D. Lasic, editors, *Gene Therapy. Therapeutic mechanisms and strategies* (Marcel Dekker Inc., New York, 2000).

[2] P. L. Felgner, M. J. Heller, P. Lehn, J.-P. Behr, and F. C. Szoka, editors, *Artificial Self-Assembling Systems for Gene Delivery* (American Chemical Society, Washington,

- DC, 1996).
- [3] A. D. Miller, *Angew. Chem. Int. Ed.*, **37**, 1768 (1998).
 - [4] R. I. Mahato and S. W. Kim, editors, *Pharmaceutical Perspectives of Nucleic Acid-Based Therapeutics* (Taylor and Francis, London and New York, 2002).
 - [5] L. Huang, M.-C. Hung, and E. Wagner, editors, *Non-Viral Vectors for Gene Therapy*, (Elsevier, San Diego, 2005).
 - [6] K. Ewert, A. Ahmad, H. M. Evans, and C. R. Safinya, *Expert Opin. Biol. Ther.* **5**, 33 (2005).
 - [7] H. Kamiya, H. Tsuchiya, J. Yamazaki, and H. Harashima, *Adv. Drug Deliv. Rev.* **52**, 153 (2001).
 - [8] J. O. Rädler, I. Koltover, T. Salditt, and C. R. Safinya, *Science* **275**, 810 (1997).
 - [9] I. Koltover, T. Salditt, J. O. Rädler, and C. R. Safinya, *Science* **281**, 78 (1998).
 - [10] O. Farago and N. Grønbech-Jensen, *J. Am. Chem. Soc.* **131**, 2875 (2009).
 - [11] O. Farago and N. Grønbech-Jensen, *Soft Matter* **7**, 4302 (2011).
 - [12] D. Haries, S. May, W. M. Gelbert, and A. Ben-Shaul, *Biophys. J.* **75**, 159 (1998).
 - [13] K. Ewert, N. L. Slack, A. Ahmad, H. M. Evans, A. J. Lin, C. E. Samuel, and C. R. Safinya, *Curr. Med. Chem.* **11**, 133 (2004).
 - [14] C. R. Safinya, *Curr. Opp. Struct. Biol.* **11**, 440 (2001).
 - [15] A. Ahmad, H. M. Evans, K. Ewert, C. X. George, C. E. Samuel, and C. R. Safinya, *J. Gene Med.* **7**, 739 (2005).
 - [16] S. Huebner, B. J. Battersby, R. Grimm, and G. Cevc, *Biophys. J.* **76**, 3158 (1999).
 - [17] M. T. Kennedy, E. V. Pozharski, V. A. Rakhmanova, and R. C. MacDonald, *Biophys. J.* **78**, 1620 (2000).
 - [18] C. L. Davey and D. B. Kell, Chapter 5 in D. Waltz, H. Berg, and G. Milazzo, editors, *Bioelectrochemistry of Cells and Tissues* (Birkhäuser, Zürich, 1995).
 - [19] J. Gimsa, T. Müller, T. Schnelle, and G. Fuhr, *Biophys. J.* **71**, 495 (1996).
 - [20] M. Kiometzis and H. Kleinert, *Phys. Lett. A* **140**, 520 (1989).
 - [21] M. Winterhalter and W. Helfrich, *J. Phys. Chem.* **96**, 327 (1992).
 - [22] In some cases (see text), these constraints may bring anions to the internal solution of the DNA array.
 - [23] S. May, D. Haries, and A. Ben-Shaul, *Biophys. J.* **78**, 1681 (2000).
 - [24] We assume no mixing with the lipids of monolayer $i = 6$, which is separated from the two external bilayers (monolayers $i = 1 - 4$) by the DNA array and the surrounding internal water layer.
 - [25] Upon attachment to the DNA, the counterions surrounding the charged macromolecules can be released, which provides an even greater driving force to this process.
 - [26] D. Harries, S. May, and A. Ben-Shaul, *Soft Matter* **9**, 9268 (2013).